

## INTERFACE TRIBOLOGY VIA NONEQUILIBRIUM MOLECULAR DYNAMICS\*

W. G. Hoover<sup>1,2</sup>, C. G. Hoover<sup>1</sup>, I. F. Stowers<sup>1</sup>, and W.J. Siekhaus<sup>1</sup>

<sup>1</sup>Lawrence Livermore National Laboratory, Post Office Box 808, Livermore, CA 94550

<sup>2</sup>Department of Applied Science, University of California at Davis-Livermore, Post Office Box 808, Livermore, CA 94550.

### ABSTRACT

By borrowing ideas from control theory, Nonequilibrium Molecular Dynamics incorporates temperature, stress, and heat flux directly into atomistic, time-reversible, deterministic equations of motion. We are applying this technique to studies of surface indentation, surface cutting, friction, ablation, and condensation. Here we describe simulations of the indentation and cutting processes using two-dimensional crystals composed of a few thousand particles.

### INTRODUCTION

The scanning tunneling microscope<sup>1</sup> now makes it possible to observe nanometer details of surfaces. Surface finishes at this same scale (below one nanometer, rms) are now directly available through precision machining single-point-diamond-turning techniques<sup>2</sup>. However, the details of the tool-tip-to-workpiece interaction, in the form of tool wear, workpiece deformation, and induced subsurface damage and residual stress, remain largely unknown. This is particularly vexing with brittle materials where the deformation may dramatically change from ductile to brittle with only a seemingly small increase in interaction load or depth of penetration.

Atomic-scale phenomena are much too detailed for continuum resolution and description to be valid. Near surfaces<sup>3,4</sup> force laws and stresses can vary on the same distance scale as the interatomic spacing. In this nanometer regime nonequilibrium molecular dynamics<sup>5</sup> is becoming a useful tool for the simulation of problems in materials science.

Today, phenomena which require an atomistic description can be simulated, provided that no more than a million degrees of freedom, corresponding to hundreds of thousands of particles, are required. With the advent of efficient parallel processors<sup>6</sup>, this limitation and the overall simulation-time limit of approximately one microsecond will gradually relax. Within these capacity and speed constraints, models are becoming more "realistic" with the development of "embedded-atom" approaches<sup>3,4,7</sup>. These approaches mimic many-body interactions with inexpensive algorithms.

Progress in microscopic equations of motion includes the incorporation of differential and integral feedback into the equations of motion, making it possible to specify temperature, stress, and heat flux for selected degrees of freedom<sup>5,8,9,10</sup>. Here we describe two-dimensional simulations of indentation and cutting using these new computational tools. Because three-dimensional simulations with a million particles correspond, in linear extent and complexity, to two-dimensional calculations with 10,000 particles, we are investigating the corresponding 10,000-particle two-dimensional crystals. Our results so far suggest that interesting effects can be seen in this size range.

## CALCULATIONS

For describing indentation, our simulated workpiece is comprised of three types of particles: boundary particles, Nosé particles<sup>5,8,9,10</sup>, and Newtonian particles. The Newtonian particles follow Newton's Second Law.

$$d(mv)/dt = dp/dt = F = ma \quad (1)$$

where  $m$  is the particle mass and  $v$ ,  $p$ ,  $F$ , and  $a$  correspond to velocity, momentum, force, and acceleration. The boundary particles form the base of the crystalline workpiece, as shown in Figure 1.

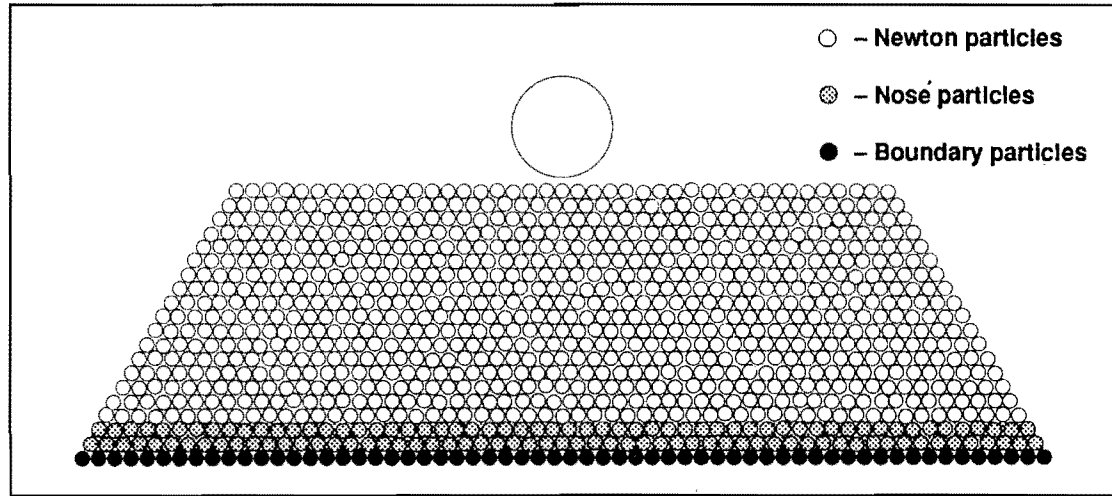


Figure 1. Time = 0.0, N = 1010 particles

These particles can be fixed or can include external viscoelastic forces which damp boundary motion and preserve the crystal's center of mass. The two rows of particles adjacent to the row of boundary particles are Nosé particles. The Nosé equations of motion,

$$d(mv)/dt = dp/dt = F - \zeta p \quad (2)$$

$$d\zeta/dt = [(p^2/mkT_{\text{average}}) - 1]/\tau^2 \quad (3)$$

include a time-dependent friction coefficient  $\zeta$  which makes it possible to specify independently the average temperature  $T_{\text{average}}$  along with a characteristic thermal relaxation time  $\tau$ . Thus the bulk workpiece temperature, relative to melting, is an independent variable.

Nosé's very recent thermostat idea (for imposing temperature control), which is required for mechanical operations on small systems, is reminiscent of Vineyard's radiation-damage boundary conditions<sup>11</sup> but is fully time-reversible. Nosé's equations, together with the usual Newtonian ones for bulk particles, and viscoelastic equations for boundary particles, are then solved numerically, using the fourth-order Runge-Kutta method.

The interatomic interactions follow a Lennard-Jones potential,

$$\phi = 4\epsilon[(\sigma/r)^{12} - (\sigma/r)^6] \quad (4)$$

or a corresponding Hooke's-Law potential, with the same curvature  $\kappa$  at the minimum in the potential energy function,  $\epsilon = -\phi(r_{\text{MINIMUM}})$ :

$$\phi = (\kappa/2)(r - r_{\text{MINIMUM}})^2 - \epsilon \quad (5)$$

$$r_{\text{MINIMUM}} = 2^{1/6}\sigma \quad (6)$$

In either case the potential is extended beyond the Lennard-Jones inflection point by a cubic spline<sup>10</sup>. Here  $r$  is the radial atomic spacing and  $\epsilon$  is the binding energy. The collision diameter is  $s$  in the Lennard-Jones model. Our indenter models use force laws based on the interatomic potential. The indenter is advanced into the workpiece using a pre-assigned, time-dependent velocity or external force, such as the example shown in Figure 2.

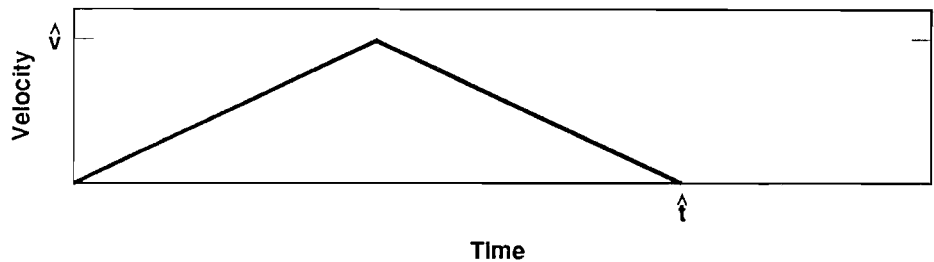


Figure 2. Piecewise-Linear Indentor velocity

For the circular indentors indicated in Figures 3 through 5, the indenter interacts with all the workpiece particles through an extended potential  $\Phi$ , with an offset Lennard-Jones form (where  $\delta$  is the magnitude of the offset):

$$\Phi(r) = \phi(r - \delta) \quad (7)$$

The availability of microscopic expressions for stress, heat flux, and temperature in terms of the individual particle coordinates and momenta<sup>5</sup> makes it possible to analyze the resulting atomistic solutions for comparison with continuum models.

## INDENTATION RESULTS

We have studied a variety of indentation problems with from 10 to 10,000 particles. We have used both prismatic and circular indentors of the type described above. The prismatic type, not shown in the Figures, was constructed of several Lennard-Jones particles moving with a common velocity. Figures 3-5 illustrate the indentation of Lennard-Jones crystals with 120-particle bases.

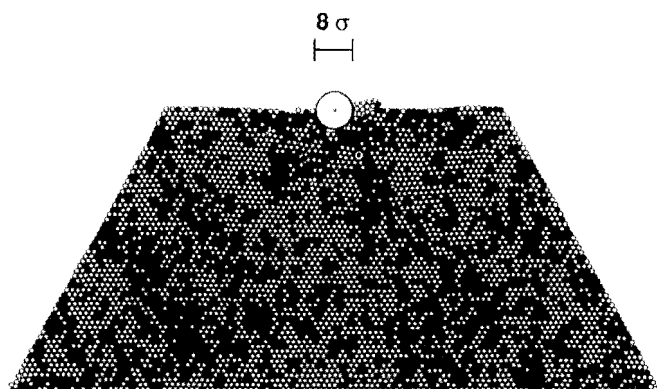


Figure 3. Lennard–Jones potential,  $N = 5430$  particles,  $kT/\epsilon = 0.15$ ,  
time =  $8.0 (m\sigma^2/\epsilon)^{1/2}$ ,  $\hat{V} = (\epsilon/m)^{1/2}$

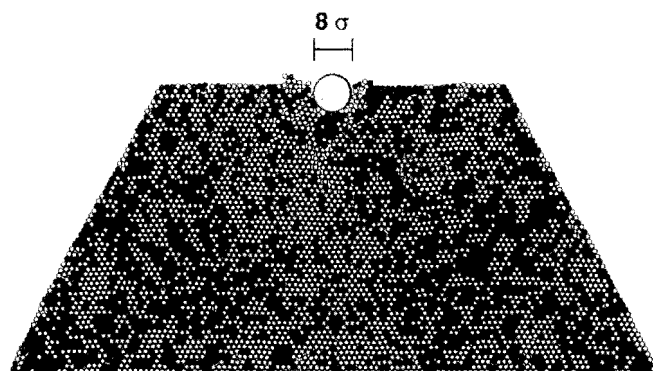


Figure 4. Lennard–Jones potential,  $N = 5430$  particles,  $kT/\epsilon = 0.30$ ,  
time =  $8.0 (m\sigma^2/\epsilon)^{1/2}$ ,  $\hat{V} = (\epsilon/m)^{1/2}$

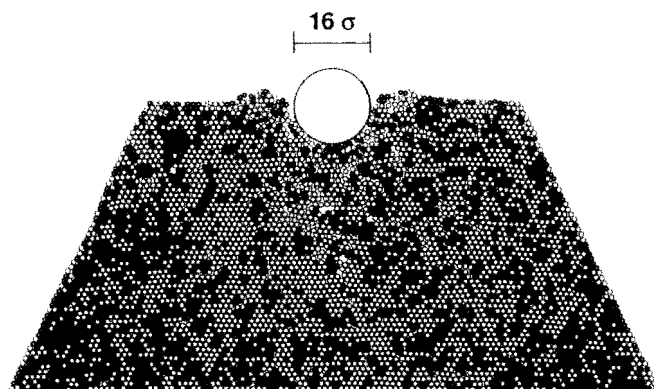


Figure 5. Lennard–Jones potential,  $N = 5430$  particles,  $kT/\epsilon = 0.30$ ,  
time =  $8.0 (m\sigma^2/\epsilon)^{1/2}$ ,  $\hat{V} = (\epsilon/m)^{1/2}$

In each of the cases shown the indenter velocity was programmed to follow the piecewise-linear time path shown in Figure 2, reaching a maximum speed

$$V_{\text{MAXIMUM}} = (\epsilon/m)^{1/2} \quad (8)$$

equal to about one-tenth the longitudinal sound speed, at half the maximum penetration distance. The penetration distance chosen corresponds to the indenter radius. The two small-indenter problems were simulated at temperatures of  $0.15(\epsilon/k)$  and  $0.30(\epsilon/k)$ . Exploratory calculations, with the indenter motionless, indicated a melting temperature of approximately  $0.42(\epsilon/k)$  for the Lennard-Jones-spline potential. Thus the simulations shown in Figures 3 and 4 correspond to relatively cold and hot samples.

The defects present in the vicinity of the indenter can be enhanced and stabilized, at any stage in the calculation, by introducing damping into the equations of motion. This causes the local thermal disorder to disappear and simplifies the cataloging of defects. The simulations can be followed in video cassette form, using software and hardware designs invented, at the NMFEECC, by Hans Bruijnes. Graphics files from a CRAY-2 are compressed, transferred to an IBM AT and edited on a graphics monitor. When the editing is complete, the monitor signal is recorded, producing the final video cassette.

In the Figures we display individual-frame snapshots of local pressure, calculated from the individual-particle potential function contributions to the pressure-volume product PV. The shaded particles make above-average contributions to the compressive stress. A general feature of the molecular-dynamics results is the development of tensile regions, even holes leading to internal cracks, directly under the indenter. It is possible that such sub-surface flaws are related to machining difficulties with materials such as molybdenum, in precision diamond turning. The indentation shape and surface finish depend upon the rate at which the tool moves.

For tool velocities comparable to the sound velocity cavities reminiscent of ballistic impact<sup>12</sup> are formed. A sufficiently small indenter can make such a small cavity that this seals itself shut again at late times.

## CUTTING RESULTS

Surface cutting can be studied by modifying the indenter path. To simulate cutting with a smooth cutter, shown in Figure 6, we compute the closest point on the wedge-shaped cutting tool and use that point as the center of a Lennard-Jones-spline force. We are in the process of exploring the sensitivity of the results, including subsurface damage, to cutter speed, temperature, as well as rake angle and shape.

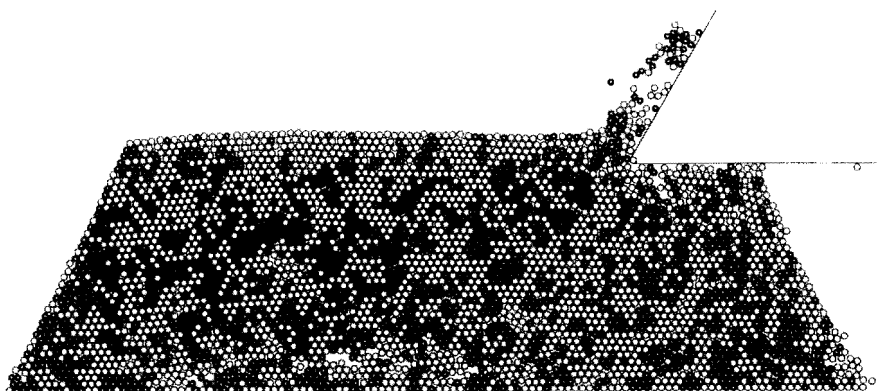


Figure 6. Lennard-Jones potential,  $N = 4020$  particles,  $kT/\epsilon = 0.30$ ,  
time =  $16.0 (m\sigma^2/\epsilon)^{1/2}$

## SUMMARY

Nonequilibrium molecular dynamics simulations of the indentation and surface cutting processes are providing insight into the subsurface flaws seen in precision diamond turning and grinding processes.

## ACKNOWLEDGMENT

\* Work performed at the Lawrence Livermore National Laboratory under the auspices of the Department of Energy pursuant to University of California-Lawrence Livermore National Laboratory Contract W-7505-Eng-48.

## REFERENCES

- <sup>1</sup> G. Binnig and H. Rohrer, *Scientific American* **253**, 50 (August, 1985).
- <sup>2</sup> R. A. Jandrisevits, *Energy and Technology Review*, UCRL-52000-87-9 (September, 1987), page 15.
- <sup>3</sup> M. S. Daw and M. I. Baskes, *Phys. Rev.* **B 29**, 6443(1984).
- <sup>4</sup> M. S. Daw and S. M. Foiles, *Phys. Rev. Letters* **59**, 2756(1987).
- <sup>5</sup> W. G. Hoover, **Molecular Dynamics, Lecture Notes in Physics**, Vol. 258 (Springer-Verlag, Berlin, 1986).
- <sup>6</sup> A. J. De Groot, S. R. Parker, and E. M. Johansson, in **SVD and Signal Processing, Algorithms, Applications, and Architectures** (North-Holland, Amsterdam, 1988), p. 439.
- <sup>7</sup> S. M. Foiles, M. I. Baskes, and M. S. Daw, *Phys. Rev.* **B 33**, 7983(1986).
- <sup>8</sup> S. Nosé, *J. Chem. Phys.* **81**, 511(1984).
- <sup>9</sup> S. Nosé, *Mol. Phys.* **52**, 255(1984).
- <sup>10</sup> W. G. Hoover, *Phys. Rev.* **A 31**, 1695(1985).
- <sup>11</sup> G. Vineyard, *J. Appl. Phys.*, cover (August, 1959).
- <sup>12</sup> B. L. Holian and D. E. Grady, *Phys. Rev. Letters* **60**, 1355(1988).